Smart Structures and Systems, *Vol. 25, No. 2 (2020) 155-167*
DOI: https://doi.org/10.12989/sss.2020.25.2.155

Real-time hybrid substructuring of a base isolated building considering robust stability and performance analysis

Muammer Avci [b], Rui M. Botelho [a] and Richard Christenson*

Department of Civil and Environmental Engineering, University of Connecticut, 261 Glenbrook Rd., Unit 3037, Storrs, CT 06269, USA

(*Received February 22, 2019, Revised July 9, 2019, Accepted January 10, 2020*)

Abstract. This paper demonstrates a real-time hybrid substructuring (RTHS) shake table test to evaluate the seismic performance of a base isolated building. Since RTHS involves a feedback loop in the test implementation, the frequency dependent magnitude and inherent time delay of the actuator dynamics can introduce inaccuracy and instability. The paper presents a robust stability and performance analysis method for the RTHS test. The robust stability method involves casting the actuator dynamics as a multiplicative uncertainty and applying the small gain theorem to derive the sufficient conditions for robust stability and performance. The attractive feature of this robust stability and performance analysis method is that it accommodates linearized modeled or measured frequency response functions for both the physical substructure and actuator dynamics. Significant experimental research has been conducted on base isolators and dampers toward developing high fidelity numerical models. Shake table testing, where the building superstructure is tested while the isolation layer is numerically modeled, can allow for a range of isolation strategies to be examined for a single shake table experiment. Further, recent concerns in base isolation for long period, long duration earthquakes necessitate adding damping at the isolation layer, which can allow higher frequency energy to be transmitted into the superstructure and can result in damage to structural and nonstructural components that can be difficult to numerically model and accurately predict. As such, physical testing of the superstructure while numerically modeling the isolation layer may be desired. The RTHS approach has been previously proposed for base isolated buildings, however, to date it has not been conducted on a base isolated structure isolated at the ground level and where the isolation layer itself is numerically simulated. This configuration provides multiple challenges in the RTHS stability associated with higher physical substructure frequencies and a low numerical to physical mass ratio. This paper demonstrates a base isolated RTHS test and the robust stability and performance analysis necessary to ensure the stability and accuracy. The tests consist of a scaled idealized 4-story superstructure building model placed directly onto a shake table and the isolation layer simulated in MATLAB/Simulink using a dSpace real-time controller.

Keywords: Real-time hybrid substructuring; base isolation; robust stability

1. Introduction

Earthquakes pose a serious threat to human lives and can causes damage to building structures.

Seismic protective systems can protect structures. Base isolation is one of the most widely used and accepted types of seismic protective systems. Seismic base isolation reduces the damage by shifting the resonant frequency of the structure below the energy content of the ground motion (Skinner *et al*. 1993, Naeim and Kelly 1999). This isolation both reduces the inter-story drifts of the superstructure and reduces the floor accelerations throughout the building. Significant research has been conducted on base isolators and high fidelity numerical models are available for base isolator devices. Long period long duration earthquakes can result in large displacements across the isolation layer and result in detrimental pounding effects. One solution is to increase the damping across the isolation layer, however, that reduces the effectiveness of the isolation, and raises concerns of damage to nonstructural components from larger amplitude and higher frequency vibration of the superstructure. This nonstructural damage can be difficult to numerically model and predict and physical testing may be desired to evaluate performance. Further, by numerically modeling the isolation layer it can be easier and less costly to examine a wide range of isolator devices for a single shake table experiment.

Shake table testing, which has been used extensively in earthquake engineering, is an experimental technique to identify the seismic behavior of a structural system (Roth and Cheney 2001). In this testing, the specimens on the shake table are subjected to excitations representative of earthquakes and the results are often considered more representative of the behavior during an actual earthquake. By combining experimental testing and numerical simulation, real-time hybrid substructure (RTHS) testing, also called real-time hybrid simulation, is an attractive alternative method to the traditional shake table testing. The RTHS approach can provide efficient and cost effective methods of considering larger systems than can be tested on the shake table (Nakashima *et al*. 1992). For example, Ashasi-Sorkhabi *et al*. (2015) conducted a study

*Corresponding author, Professor,
E-mail: Richard.christenson@uconn.edu
[a] Ph.D., E-mail: rui.botelho@uconn.edu
[b] Ph.D. Student, E-mail: muammer.avci@uconn.edu

ISSN: 1738-1584 (Print), 1738-1991 (Online)

implementing RHTS with a shake table where a tuned liquid damper (TLD) was physically tested on a shake table and the building structure below the TLD was numerically modeled. Additionally, Zhang *et al*. (2017) demonstrated RTHS for a building with a mid-height isolation layer.

Early research demonstrated RTHS to be a useful tool in earthquake and structural engineering (Nakashima and Masaoka 1999, Darby *et al*. 1999, Dimig *et al*. 1999, Horiuchi *et al*. 1999). Recent advances in RTHS have been made possible by increased computing power, digital signal processing hardware/software, and hydraulic actuation. RTHS allows a structural dynamic system to be partitioned into physical and numerical substructures. The substructure of interest is physically tested, while the substructure that is better understood is simulated in real-time using analytical or numerical models. In an RTHS test, the numerical and experimental substructures communicate together in real-time by transferring displacement and force signals through a feedback loop using controlled actuation and sensing. This paper proposes an RTHS test configuration where the building superstructure is the physical substructure and isolation layer is the numerical superstructure. This accounts for uncertainty in acceleration levels and possible damage in the superstructure (the physical substructure) and leverages the availability of numerical models for isolators and dampers considered in the base isolation (the numerical substructure). This choice of substructuring will facilitate the exploration of various isolation layer configurations. Fig. 1 shows a block diagram of a closed loop RTHS test for a base isolated structure. At a given time-step, loading, including ground displacement and velocity and base shear, is applied to the numerical substructure to determine the numerical displacement, x_n, to be imposed on the physical substructure. The numerical displacements are then fed into a controller to identify the command displacements, x_c, to send to the hydraulic actuator to insure the displacement imposed upon the physical substructure, x_d, is close in magnitude and phase to the desired numerical displacement. The measured restoring force, V_b, of the physical substructure, once displacement, is fed back into the numerical substructure, along with the ground displacement and velocity of the next time step, to compute the numerical displacements for the next time step. This loop continues, marching through time at the discrete time steps, until the duration of the test is completed.

Since RTHS involves a feedback loop, the inherent time delay of the actuator transfer system can lead to inaccuracy in the actuator tracking and potential instability during closed-loop testing. The effect of time delay on RTHS testing was initially considered by Horiuchi *et al*. (1996), who showed that actuator delay can cause an increase in the total energy, which is equivalent to introducing negative damping into the system. When the negative damping is larger than the total system damping, the RTHS test will become unstable. Previous RTHS tests without actuator delay compensation had been performed for systems with very low natural frequencies and high damping to achieve stability. There are also other sources of time delay in a RTHS test, including communication delays of the various electrical signals and computational delays for solving the numerical substructure. These time delays are generally much smaller than the inherent time delay of the actuator transfer system.

To improve the closed-loop stability and performance of RTHS, researchers have developed a variety of techniques for compensating the time delay or more generally the frequency dependent dynamics of the actuator transfer system. The techniques range from polynomial extrapolation in Horiuchi *et al*. (1999) and inverse compensation in Chen and Ricles (2009) to reduce the actuator delay as well as adaptive techniques in Chen and Ricles (2010) and Chae *et al*. (2013). Carrion and Spencer (2007) used a controls approach to develop model-based feedforward-feedback control to compensate the frequency-dependent magnitude and phase of the actuator dynamics. Phillips and Spencer (2012) extended this approach with a more accurate feedforward inverse of the actuator dynamics and added linear-quadratic Gaussian (LQG) feedback control. Christenson and Lin (2008) employed virtual coupling to balance closed-loop stability and performance in RTHS testing of large-scale MR dampers. Gao *et al*. (2013) developed an H-infinity robust loop-shaping controller to compensate the actuator dynamics for RTHS testing of lightly damped steel frame structures. Nakata and Stehman (2014) introduced a model-based actuator delay compensation and a force correction technique to achieve desired interface acceleration tracking. Shi *et al*. (2015) introduced a Kalman filter to cancel the noises in the measured actuator displacement for enhanced performance. Lin *et al*. (2015) illustrate the use of the predictive

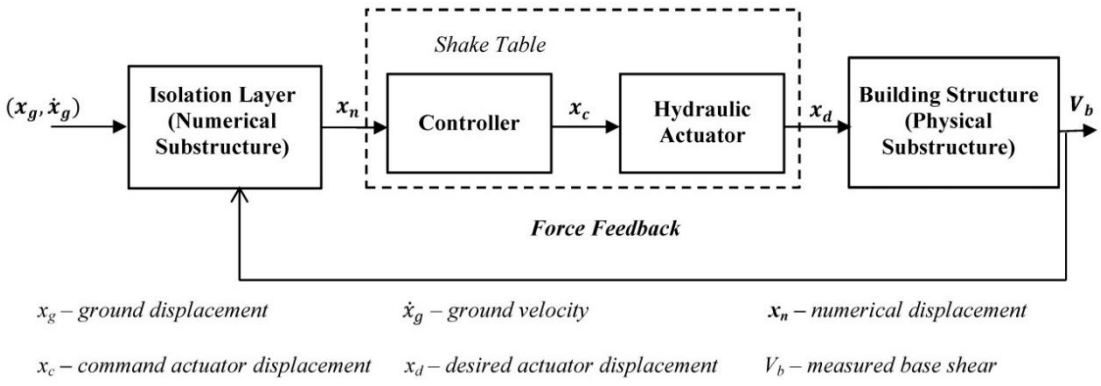

Fig. 1 Block diagram for real-time hybrid substructuring of a base isolated structure

indicators for an RTHS, and effectiveness and accuracy of the approach examined. Further, Ou *et al*. (2015) describe a new actuator control algorithm for achieving design flexibility, robustness, while Maghareh *et al*. (2016) introduced a rate-transitioning and compensation technique that enables implementation of multi-rate RTHS. The ultimate goal of these compensation techniques is to provide effective displacement tracking of the actuator transfer system over the desired frequency range of the RTHS test, called the control band. This prior research to improve the dynamics of the actuator transfer system has been largely successful in this regard.

Stability and performance analysis is an important tool for understanding the effect of actuator time delay on the stability behavior and accuracy of RTHS. This information is especially useful in guiding the compensation design of the actuator transfer system to reduce its inherent time delay and provide closed-loop stability and performance. Wallace *et al*. (2005) studied the effect of actuator time delay using delay differential equation (DDE) modeling of a single degree of freedom (SDOF) RTHS system comprised of a physical stiffness coupled to an analytically modeled mass-spring oscillator. Kyrychko *et al*. (2006) applied a similar approach to identify the critical time delays for RTHS of a physical pendulum coupled to an analytical mass-spring oscillator, using neutral DDE's. Botelho *et al*. (2013) presented an exact stability analysis technique for single-actuator RTHS of 1-DOF and 2-DOF mass-spring systems to quantify the critical time delays. Although these stability analysis techniques provide insight into the stability behavior of RTHS, they assume pure time delay for the actuator dynamics and are limited to lumped parameter descriptions of the numerical and physical substructures.

While progress has been made in the development of stability analysis techniques for RTHS, performance analysis has received less attention. Maghareh *et al*. (2014) recently proposed a predictive performance indicator for SDOF RTHS to assess the effect of actuator time delay as well as computational and communication delays on the accuracy of RTHS. The predictive performance indicator also provides insight on the effect of mass, stiffness, and damping partitioning of the physical and numerical substructures.

The robust stability and performance analysis method considered here involves casting the actuator dynamics of the RTHS feedback loop as a multiplicative uncertainty and then applying the small gain theorem to derive sufficient conditions for robust stability and performance for RTHS. Gawthrop *et al*. (2007) was first to consider robust stability in RTHS, in which they used the robust stability criterion in Goodwin *et al*. (2001) to study the stability of single-actuator RTHS, but assumed a pure time delay for the actuator transfer system. Recognizing the versatility of this approach, this paper presents an extension of robust stability analysis to consider robust performance and multi-actuator RTHS. Unlike previous stability analysis techniques which assume pure time delay, this method accommodates the linearized modeled or measured frequency-dependent magnitude and phase of the actuator dynamics as well as linearized modeled or measured frequency response functions of the physical substructure.

2. Robust stability and performance analysis

The RTHS feedback loop is shown in Fig. 2 for the seismically excited base isolated building. For the numerical substructure, the transfer function $N_{XnXg}(s)$ relates input numerical displacement, x_g, to output displacement responses, x_n, where s is the Laplace variable. The transfer function $N_{XnFr}(s)$ relates input restoring forces, f_r, to output displacement responses, x_n, in the numerical substructure. For the physical substructure, the transfer function $P_{FrXa}(s)$ relates input actuator displacements, x_a, to measured restoring forces, f_r.

To enforce force equilibrium, the measured restoring forces from the physical substructure are fed back into the numerical substructure, applied as equal and opposite input forces. To enforce displacement compatibility, the actuator transfer system with compensation, $\hat{A}(s)$, is used in implementing an RTHS test to impose the displacement response of the numerical substructure onto the physical substructure. It should be noted that the above block diagram assumes that the sensor dynamics for the measured restoring force of the physical substructure are negligible. With appropriate selection of force sensors with constant magnitude and little phase distortion at low frequencies, this assumption is reasonable for the control band below 40 Hz of a typical RTHS test.

From the above block diagram, the closed-loop response

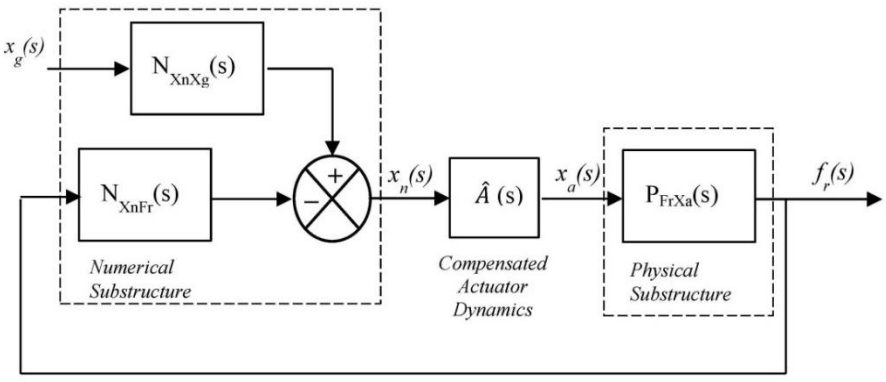

Fig. 2 The RTHS feedback loop for a seismically excited base isolated building

for the numerical displacement is

$$\{x_n(s)\} = [I + N_{XnFr}(s)P_{FrXa}(s)\hat{A}(s)]^{-1}[N_{XnXg}]\{x_g(s)\} \quad (1)$$

where {.} denotes a vector and [.] a matrix quantity, such that the formulation captures both single and multi-actuator RTHS. The closed-loop response for the measured restoring force is

$$\{f_r(s)\} = [I + N_{XnFr}(s)P_{FrXa}(s)\hat{A}(s)]^{-1} [P_{FrXa}(s)]\,[\hat{A}(s)]\,[N_{XnXg}]\{x_g(s)\} \quad (2)$$

The sensitivity matrix is defined as

$$S(s) = [I + L(s)]^{-1} \quad (3)$$

where, $L(s) = N_{XnFr}(s)P_{FrXa}(s)\hat{A}(s)$ is the loop gain for RTHS. The complimentary sensitivity matrix is then defined as

$$T(s) = [I + L(s)]^{-1}[L(s)] \quad (4)$$

Since the actuator dynamics, $\hat{A}(s)$, is in the feedback path, the presence of time delay in the actuator transfer system will have a destabilizing effect on the RTHS closed-loop response. Using concepts from robust stability theory for feedback control (Goodwin *et al*. 2001), the compensated actuator dynamics is cast as a multiplicative uncertainty, as illustrated in Fig. 3, by following a similar procedure as described previously.

The compensated actuator dynamics matrix $[\hat{A}(s)]$ is related to the uncertainty matrix $[\Delta(s)]$ by

$$[\hat{A}(s)] = [\Delta(s)] + [I] \quad (5)$$

Considering that the compensated actuator dynamics, $[\hat{A}(s)]$, can be a directly measured frequency response function, the uncertainty matrix, $[\Delta(s)]$, is determined by rearranging (5), as

$$[\Delta(s)] = [\hat{A}(s)] - [I] \quad (6)$$

Substituting Eq. (6) into Eq. (5), the complimentary sensitivity matrix becomes

$$[T(s)] = [I + N_{XnFr}(s)P_{FrXa}(s)(\Delta(s) + I)]^{-1} [N_{XnFr}(s)][P_{FrXa}(s)][\Delta(s) + I] \quad (7)$$

Expanding as

$$[T(s)] = \begin{bmatrix} I + N_{XnFr}(s)P_{FrXa} \\ +N_{XnFr}(s)P_{FrXa}(s)\Delta(s) \end{bmatrix}^{-1} [N_{XnFr}(s)][P_{FrXa}(s)][\Delta(s) + I] \quad (8)$$

and then factoring out $[I + N_{XnFr}(s)P_{FrXa}]^{-1}$ leads to

$$[T(s)] = [I + T_0(s)\Delta(s)]^{-1}[T_0(s)][\Delta(s) + I] \quad (9)$$

where the nominal complimentary sensitivity matrix is defined as

$$[T_0(s)] = [I + N_{XnFr}(s)P_{FrXa}]^{-1} [N_{XnFr}(s)][P_{FrXa}(s)] \quad (10)$$

Note that the presence of actuator dynamics introduces $[T_0(s)\Delta(s)]$ in the denominator of (9). For the single actuator system considered for the RTHS base isolated test in this paper, the matrix $[T_0(s)\Delta(s)]$ becomes the scalar quantity $T_0(s)\Delta(s)$. When the $T_0(s)\Delta(s)$ term approaches -1, the complimentary sensitivity matrix is unbounded and the closed loop RTHS system will go unstable. By employing the small gain theorem, the sufficient condition for robust stability for the single actuator RTHS case is

$$|T_0(s)\Delta(s)| < 1 \quad (11)$$

where, | | denotes the maximum magnitude over the RTHS control band and $T_0(s)$ is given in (10) from modeled numerical and measured physical frequency response function substructures, and $\Delta(s)$ is given in (6) as calculated from the measured compensated actuator frequency response functions.

The robust stability criterion alone does not ensure robust performance of the RTHS system in the presence of actuator dynamics. Goodwin *et al*. (2001) suggests one approach for robust performance is to ensure that the actual sensitivities are close to the nominal sensitivities by

$$|T_0(s)\Delta(s)| \ll 1 \quad (12)$$

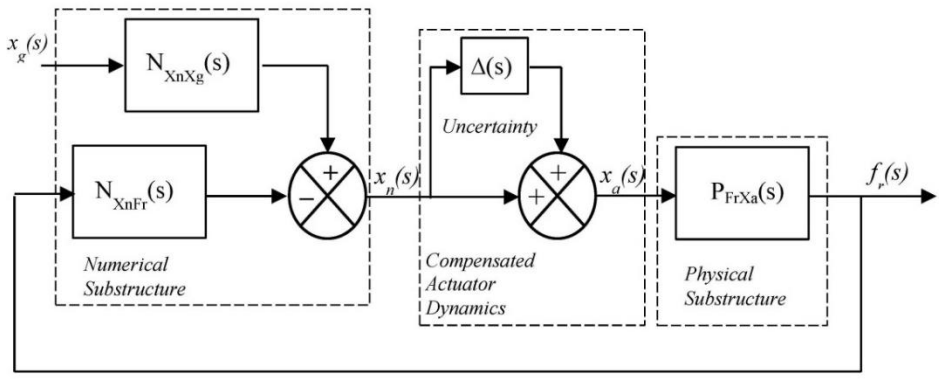

Fig. 3 RTHS feedback loop with compensated actuator dynamics cast as multiplicative uncertainty

The above robust performance criterion in (12) is similar but more restrictive than the robust stability criterion in (11). The sufficient conditions in (11) and (12) provide the basis for a new robust stability and performance analysis method for both single and multi-actuator RTHS. The robust stability and performance criterion for RTHS are similar to those for MIMO feedback control with plant uncertainty in Goodwin *et al*. (2001). The differences are in the expressions for the nominal complimentary sensitivity and uncertainty.

The robust stability and performance analysis involves a singular value decomposition of the nominal complimentary sensitivity matrix multiplied by the uncertainty matrix at each frequency. Unlike previous stability analysis techniques which assume pure time delay and lumped parameter descriptions, this method better captures the actual frequency dependence of the magnitude and phase lag of the actuator dynamics as well as accommodates more complex representations of the numerical and physical substructures.

To extend this approach for multi actuator systems, (11) and (12) are arrived at considering MIMO robust stability (Skogestad and Postlethwaite 2005) to derive similar sufficient conditions employing matrix norms, particularly the maximum singular value, which defines the principal gain of a matrix. The sufficient condition for MIMO robust stability is

$$\|[T_0(s)\Delta(s)]\|_\infty < 1 \tag{13}$$

and the sufficient condition for MIMO robust performance is

$$\|[T_0(s)\Delta(s)]\|_\infty \ll 1 \tag{14}$$

where $[T_0(s)] = [I + G_0(s)K(s)]^{-1}[G_0(s)][K(s)]$ and $[\Delta(s)] = [G_0(s)]^{-1}[G(s)] - [I]$

In the above expressions, $\|\ \ \|_\infty$, denotes the maximum singular value over the control band. $[T_o(s)]$ is the nominal complimentary sensitivity matrix and $[\Delta(s)]$ is the uncertainty matrix. Further, for nonlinearities in the numerical and/or physical components as well as more complex actuator control strategies, the robust stability and performance is observed to provide good estimates of stability and performance when linearized models or frequency response functions taken at the operating points are employed in the analysis. From prior experience, the inequality conditions of (12) and (14) can be assumed in practice to be an order of magnitude less than unity, 0.1 or -20 dB.

3. RTHS test Setup

To conduct RTHS for a base isolated structure, a model is desired where the isolation layer and building structure are substructures, interfaced appropriately. Fig. 4 illustrates the substructuring employed for the RTHS test setup of a base isolated a four story structure where the physical building is mounted on uniaxial shake table and the isolation layer is a numerical model.

In this setup, a dSPACE real-time digital signal processor (DSP) is utilized to simulate the numerical substructure. The dSpace DSP is programmed on a host computer using the Simulink library and transferred to dSPACE using the MATLAB Real-Time Workshop. The displacement command from the numerical substructure is compensated to account for the dynamics of the hydraulic actuator of the shake table and sent to an analog servo controller commanding the hydraulic actuator to enforce the base displacements onto the physical substructure. The base shear of the building is measured in the physical substructure as the restoring force. The measured restoring force signal is fed back into the dSPACE DSP to complete the RTHS feedback loop. A Data Physics SignalCalc

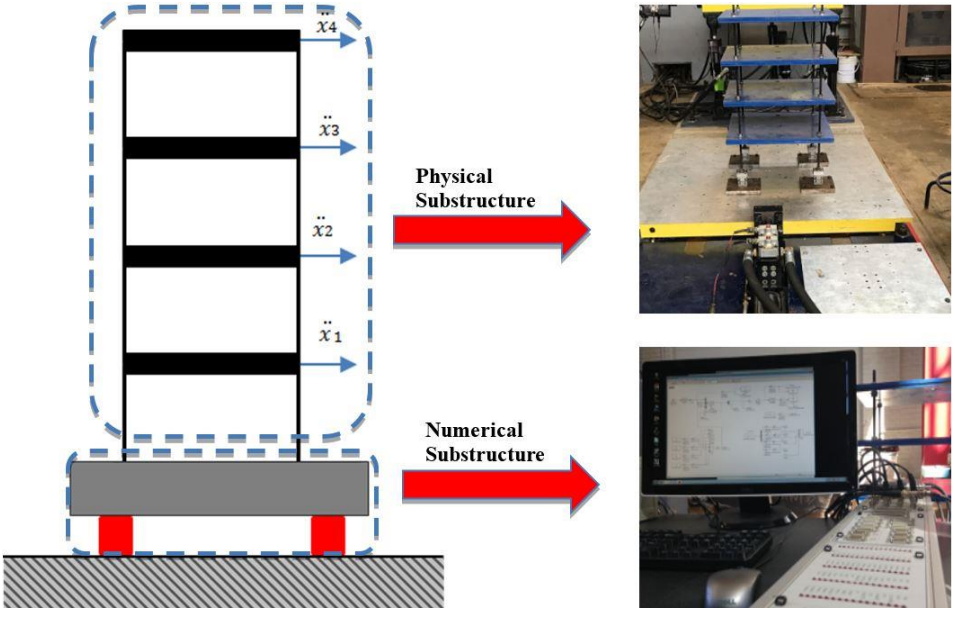

Fig. 4 RTHS test configuration of a base isolated four story building structure

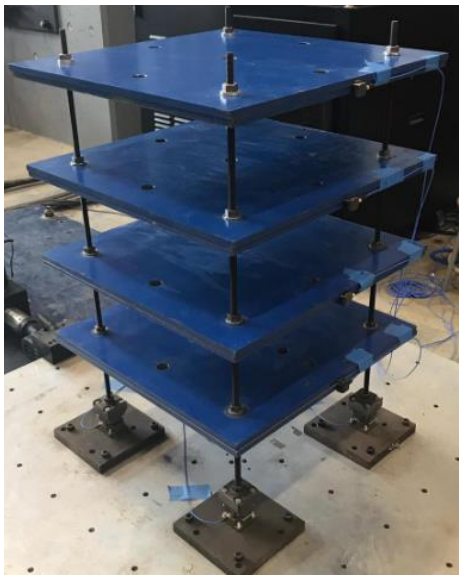

Fig. 5 The four story physical substructure

Mobilyzer dynamic signal analyzer is utilized to acquire the physical and numerical data for evaluation. The base isolated building considered in this research consists of a single degree-of-freedom (SDOF) numerical substructure corresponding to the isolation layer of the building and a physical substructure that represents a 4-story superstructure. The superstructure is modeled for validation purposes as a four degree-of-freedom (4DOF) lumped mass system. These substructures are discussed subsequently.

3.1 Physical substructure

A scaled and idealized 4-story superstructure building is considered in this study as the physical substructure, as shown in Fig. 5. The building is 32 inches (in) tall and 24 in by 24 in in plan. Four 0.5 in diameter steel threaded rods are used as columns, with the length of each fixed-fixed column between the stories set to 6 in. The effective diameter of the threaded rods is 3/8 in (0.375 in) after taking into account the threads role in the moment of inertia. Further, the presence of the force transducers at the base of the structure added an effective length to the columns at the base, such that the first story columns are assumed have a length of 8 in. The floors consist of 2 stacked 24 in square 1 in thick steel plates held in place with nuts and washers on the column threaded rods.

The base shear of the physical superstructure, V_b, can be determined directly by using the sum of the x-axis measurements of four PCB (model: 261A02) three component ICP triaxle force transducers attached at the base of each column of the building. For larger test specimens, this approach may not be feasible. As such, the base shear can be *calculated* by summing the product of the calculated mass and measured acceleration at each of the four stories of the building. Fig. 6 shows a comparison of these two approaches, to verify the method of calculating base shear from story accelerations. A band limited white noise base excitation is used with a bandwidth of 0 to 40 Hz. In the figure, the two approaches yield a similar frequency response function between the ground displacement input and base shear of the superstructure. The base shear for the RTHS test is determined from the story accelerometers.

While the building is physically tested in the laboratory, for validation it is useful to develop a numerical model of the superstructure. The column stiffness is calculated using material and geometric properties of the threaded rods such that the story stiffness of the ith story is $k_i = 4(12EI)/h^3$ where, E is the modulus of elasticity of steel (29,000 ksi), $I = \frac{\pi}{4}\left(\frac{d}{2}\right)^4$ is the moment of inertia of a single threaded

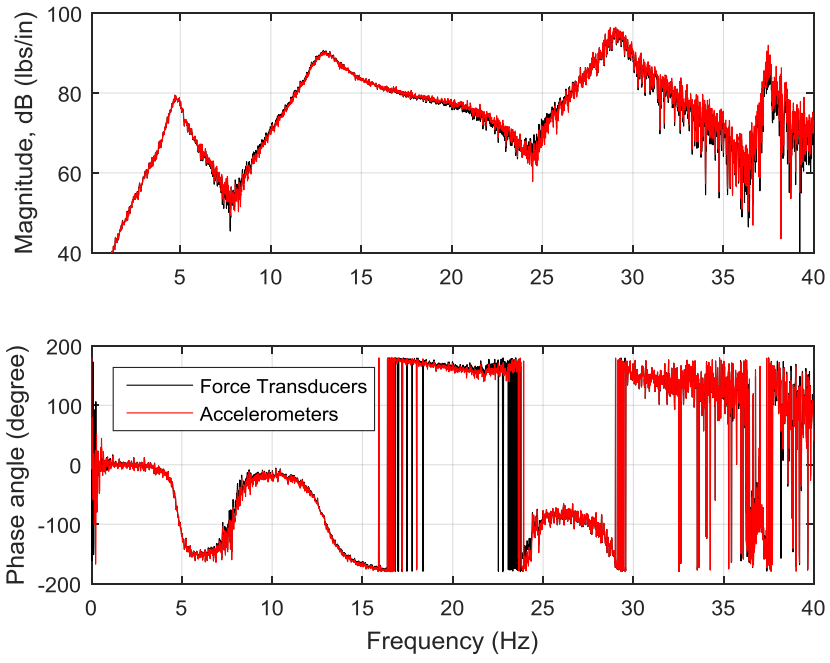

Fig. 6 Measured and calculated frequency response functions of base shear to base displacement

rod, d is the effective diameter of the rod, and h is the length of the column at each story. The mass of the ith floor, m_i, is calculated from the mass of the two steel plates and portion of the columns (neglecting the mass of the nuts and washers) to be 0.4222 lbs-s2/in (a weight of 81.5 lbs per story).

The equations of motion for the physical building model, written in matrix form where the subscript p denotes the physical substructure, are

$$\mathrm{M_p}\ddot{\mathrm{X}}_\mathrm{p} + \mathrm{C_p}\dot{\mathrm{X}}_\mathrm{p} + \mathrm{K_p}\mathrm{X}_p = -\Gamma \mathrm{M_p}\ddot{x}_b{}^a \tag{15}$$

where $\mathrm{M_p}$, $\mathrm{C_p}$, and $\mathrm{K_p}$ are and the mass, damping and stiffness matrices of the building structure, respectively, $\ddot{\mathrm{X}}_\mathrm{p}$ is a vector of displacements of the physical building superstructure where [.] indicates a derivative with respect to time, the vector Γ defines the loading of the ground motion, and $\ddot{x}_b{}^a$ is the absolute acceleration of the base of the structure (i.e., the ground acceleration for a fixed base structure), such that

$$M_p = \begin{bmatrix} m_1 & 0 & 0 & 0 \\ 0 & m_2 & 0 & 0 \\ 0 & 0 & m_3 & 0 \\ 0 & 0 & 0 & m_4 \end{bmatrix}$$

$$K_p = \begin{bmatrix} k_1 + k_2 & -k_2 & 0 & 0 \\ -k_2 & k_2 + k_3 & -k_3 & 0 \\ 0 & -k_3 & k_3 + k_4 & -k_4 \\ 0 & 0 & -k_4 & k_4 \end{bmatrix}$$

$$X_2^a = \begin{bmatrix} x_1^a \\ x_2^a \\ x_3^a \\ x_4^a \end{bmatrix} \qquad \Gamma = \begin{bmatrix} 1 \\ 1 \\ 1 \\ 1 \end{bmatrix}.$$

The damping matrix is determined from an assumption of modal damping, with 1%, 2%, 1% and 0.2% damping in the first, second, third and fourth modes, respectively, based on measured frequency response functions of the fixed base structure.

3.2 Numerical substructure

A numerical model is developed for the isolation layer. This model is the numerical substructure in the RTHS tests and a dSPACE real-time digital signal processor (DSP) board (dSPACE real-time controller) is utilized to simulate the numerical substructure. The dSPACE real-time controller is programmed on a host computer using the Simulink library and transferred to dSPACE using the MATLAB Real-Time Workshop.

The isolation layer is simplified to consist of a base mass, $\mathrm{m_b}$, isolator stiffness, $\mathrm{k_b}$, and isolator damping, $\mathrm{c_b}$. This model can be extended to provide more complex and nonlinear realizations of the isolation layer as desired, although for the purposes of this study a linear isolation layer is desired. The mass of the isolation layer is characterized by the mass ratio, defined as $\mu = {m_b}/{\sum_{i=1}^{4} m_i}$, and is set to mass ratios of m = 1, m = 2 and m = 15 in this paper. The natural frequency of the base isolated structure, defined as $\omega_b = \sqrt{{k_b}/{(m_b + \sum_{i=1}^{4} m_i)}}$, is $0.33\ Hz$, such that the stiffness of the base isolation layer is calculated as $k_b = {\omega_b}^2(m_b + \sum_{i=1}^{4} m_i)$. The damping ratio of the isolation layer is 5%, $\zeta = 0.05$ and the damping coefficient of the isolation layer is calculated as $c_b = 2\zeta(m_b + \sum_{i=1}^{4} m_i)\omega_b$. For implementation in RTHS, the equation of motion for the isolation layer should have as inputs the ground motion and the base shear of the superstructure it is supporting, and the output must be the absolute displacement of the isolation layer. As such the equation of motion is written as

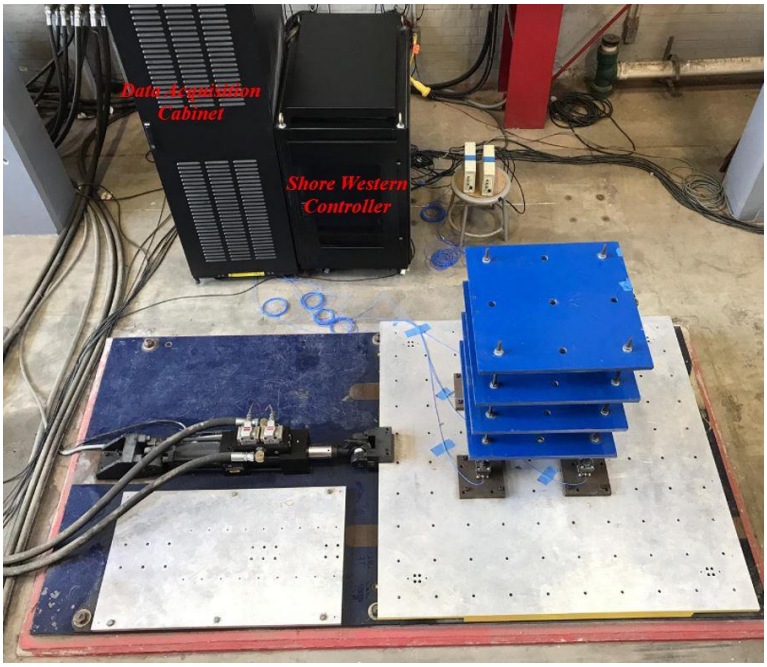

Fig. 7 Shake table with the physical substructure

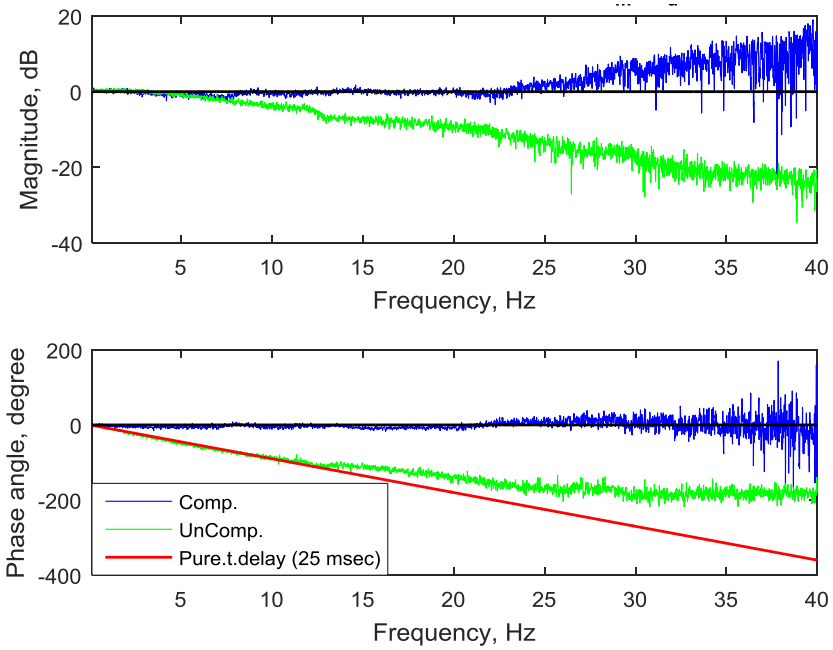

Fig. 8 Compensated versus uncompensated frequency response function of the shake table transfer system

$$m_b \ddot{x}_b{}^a + c_b \dot{x}_b{}^a + k_b x_b{}^a = c_b \dot{x}_g + k_b x_g + V_b. \quad (16)$$

3.3 Transfer system

The transfer system, or mechanism to impart displacements onto the physical specimen, in this research is a medium-scale uniaxial seismic simulator with a 1.52 by 1.52 m (60 in by 60 in) slip table and a ±150 mm (6 in) available stoke. A picture of the shake table with physical substructure mounted is shown in Fig. 7. A linear-variable-differential-transformer (LVDT) is used to measure shake table displacement. A Shore Western digital controller is used to command the-hydraulic actuator to enforce the displacements from the numerical model.

The frequency-dependent dynamics of the shake table transfer system in the RTHS feedback loop can lead to inaccuracy and potential instability. Fig. 8 provides the measured frequency response function of the servo-hydraulic actuator for the uniaxial shake table prior to any compensation. The input (x_d) is desired displacement while the output (x_m) is measured table displacement. The actuator is excited with a band limited white noise command for the desired displacement with a bandwidth of 0 to 40 Hz. Fig. 8 shows an approximate 25 msec. apparent time delay of the uncompensated transfer system.

A model-based feedforward inverse compensation method is used to improve the actuator frequency response function to ensure system stability and accuracy. In this approach the frequency response function is curve fit with numerator and denominator polynomials of the transfer function. The transfer function is made to be proper by adding additional dynamics above the bandwidth of interest and the inverted to be used as the compensator. This basic approach is sufficient for the testing conducted here. Fig. 8 shows a comparison of the compensated and uncompensated frequency response functions.

4. Results

4.1 Numerical analysis of base isolate building structure

The purpose of base isolation is to reduce the seismic response of the superstructure. To observe this effect, the magnitude of the frequency response function for the superstructure absolute accelerations to input ground acceleration are considered. Fig. 9 shows the frequency response functions for the four stories of the superstructure for three distinct cases: (1) a fixed base structure, the superstructure itself; (2) a base isolated structure with a mass ratio of 2; and (3) a base isolated structure with a mass ratio of 15.

As observed in Fig. 9, the fixed base structure (superstructure) has resonant frequencies around 5.2 Hz, 17 Hz, 28 Hz and 36 Hz. Also observed in Fig. 9, the isolation reduces the magnitude of the superstructure absolute acceleration response above the isolation frequency by approximately 35 dB (over a 98% reduction) while adding a fifth resonant peak at 0.33 Hz (3 second period), while slightly shifting the frequencies of the resonant frequencies of the superstructure, most noticeably the first resonant frequency of the superstructure shifting from 5.2 Hz to 6.3 Hz for a mass ratio of 2 and 5.35 Hz for a mass ratio of 15. It can be observed that while the added mass at the isolation layer does affect the resonant frequencies of the superstructure, the magnitudes and phase of the isolated system, above the isolation frequency is minimal. The resonant peak at the isolation frequency, 0.33 Hz, is increased from 14 to 18 dB for the increased mass ratio. These effects will be observed for the experimentally collected RTHS test results.

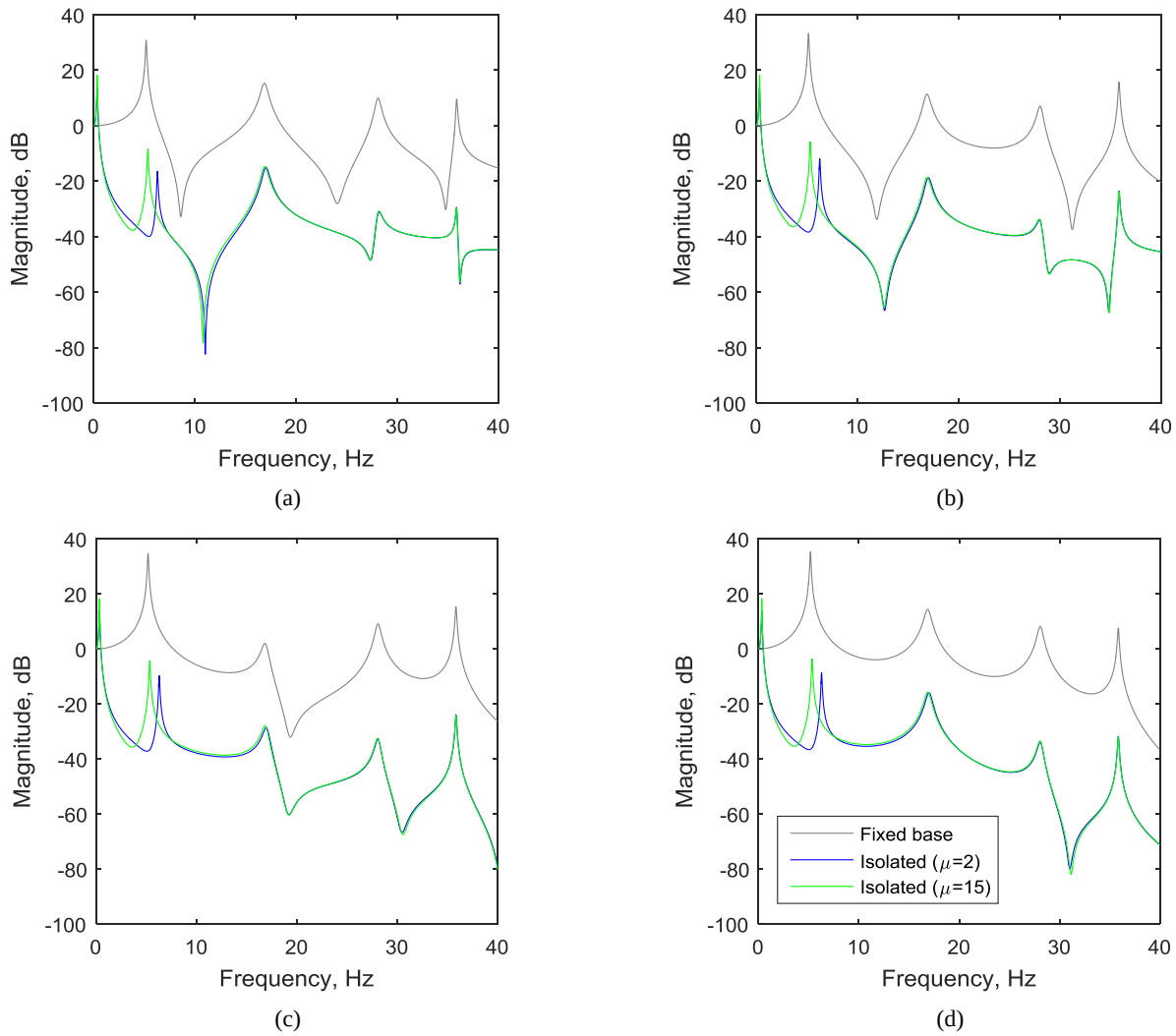

Fig. 9 Numerical transfer functions of absolute story acceleration to ground acceleration for fixed-base and base isolated 4-story buildings: (a) first floor; (b) second floor; (c) third; (d) fourth [top] floor

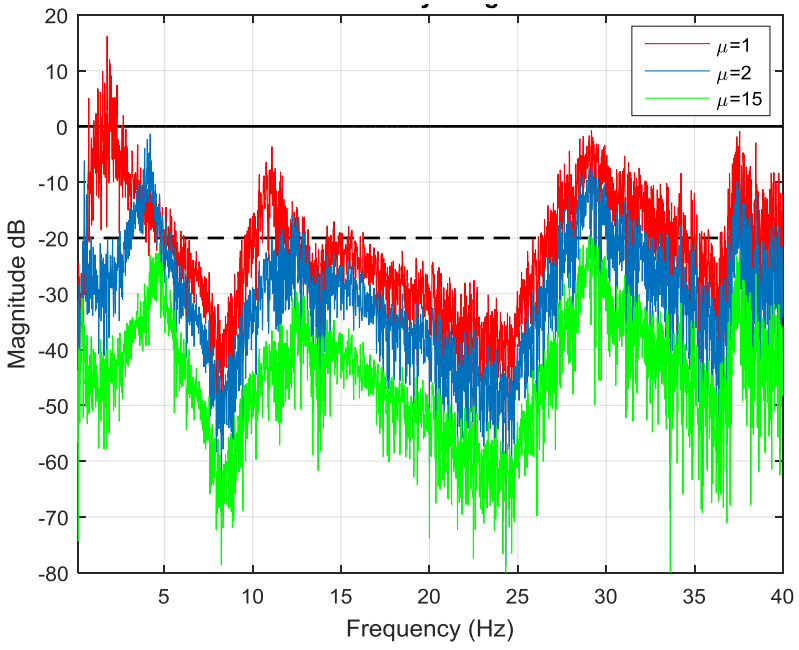

Fig. 10 Robust stability and performance margins of base isolated four story structure

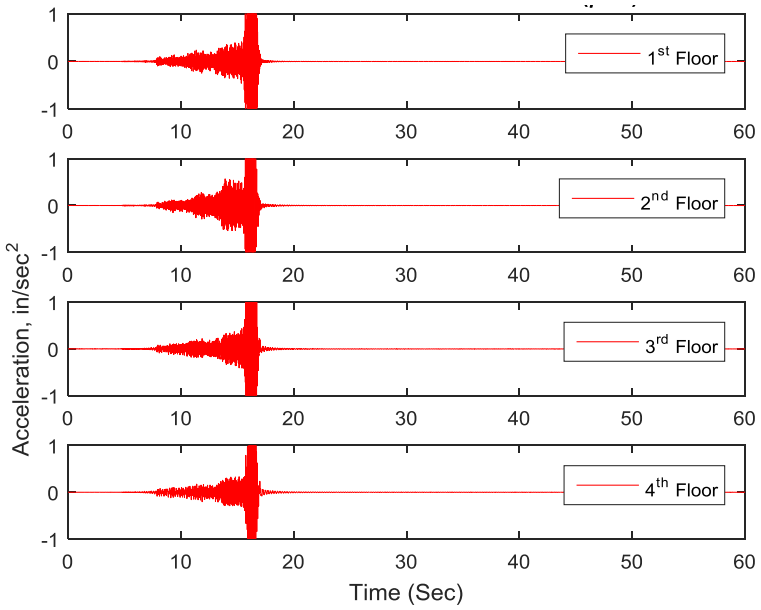

Fig. 11 Time histories of floor acceleration for unstable mass ratio of 1 (μ = 1)

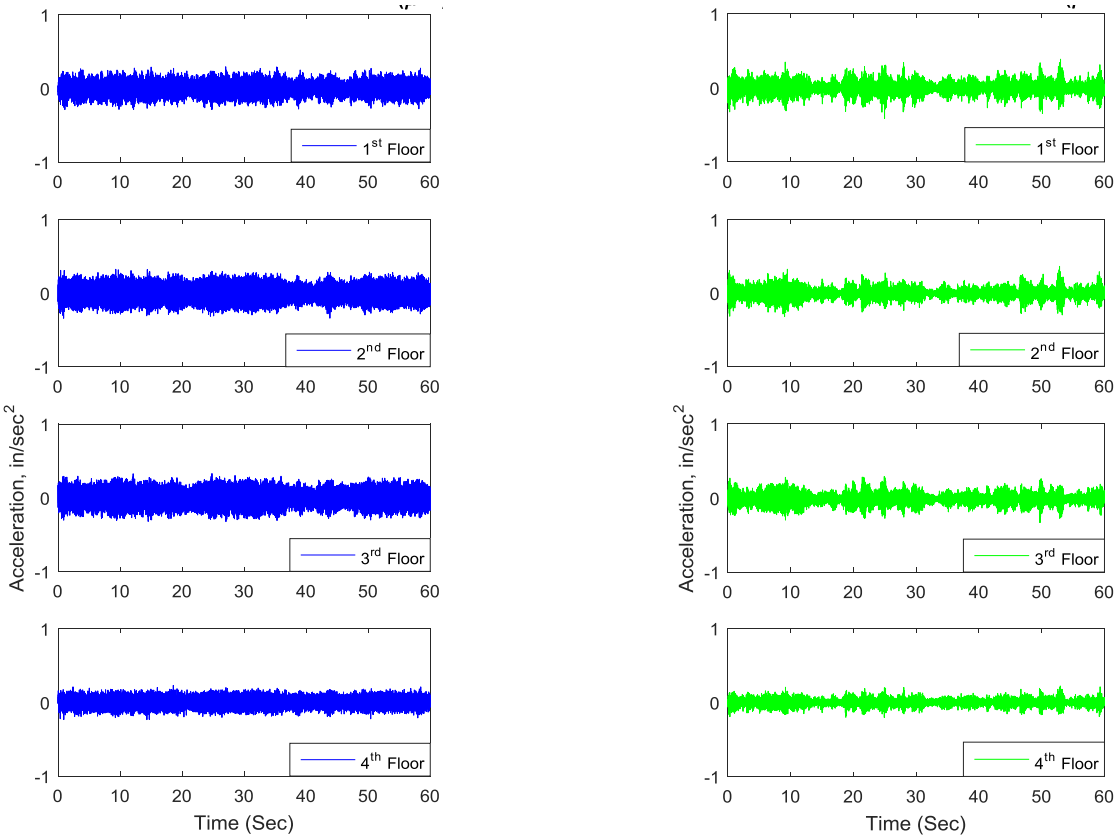

Fig. 12 Time histories of floor acceleration for mass ratios of 2 (left, μ = 2) and 15 (right, μ = 15)

4.2 Stability and performance analysis result

Prior to conducting the RTHS test, the robust stability and performance margins are determined using the experimentally measured frequency response functions of the physical superstructure, $P_{FrXa}(w)$, and compensated actuator, $\hat{A}(\omega)$, and the numerically calculated frequency response function of the numerical isolation layer $N_{XnFr}(w)$. Note, that the frequency response function, $P_{FrXa}(w)$, is the measured frequency response function in Fig. 6 and the compensated actuator frequency response function, $\hat{A}(\omega)$, is the measured frequency response function shown in Fig. 8. The Laplace variable in (6), (10), (11) and (12) can be exchanged with the frequency variable, where $s = jw$, and

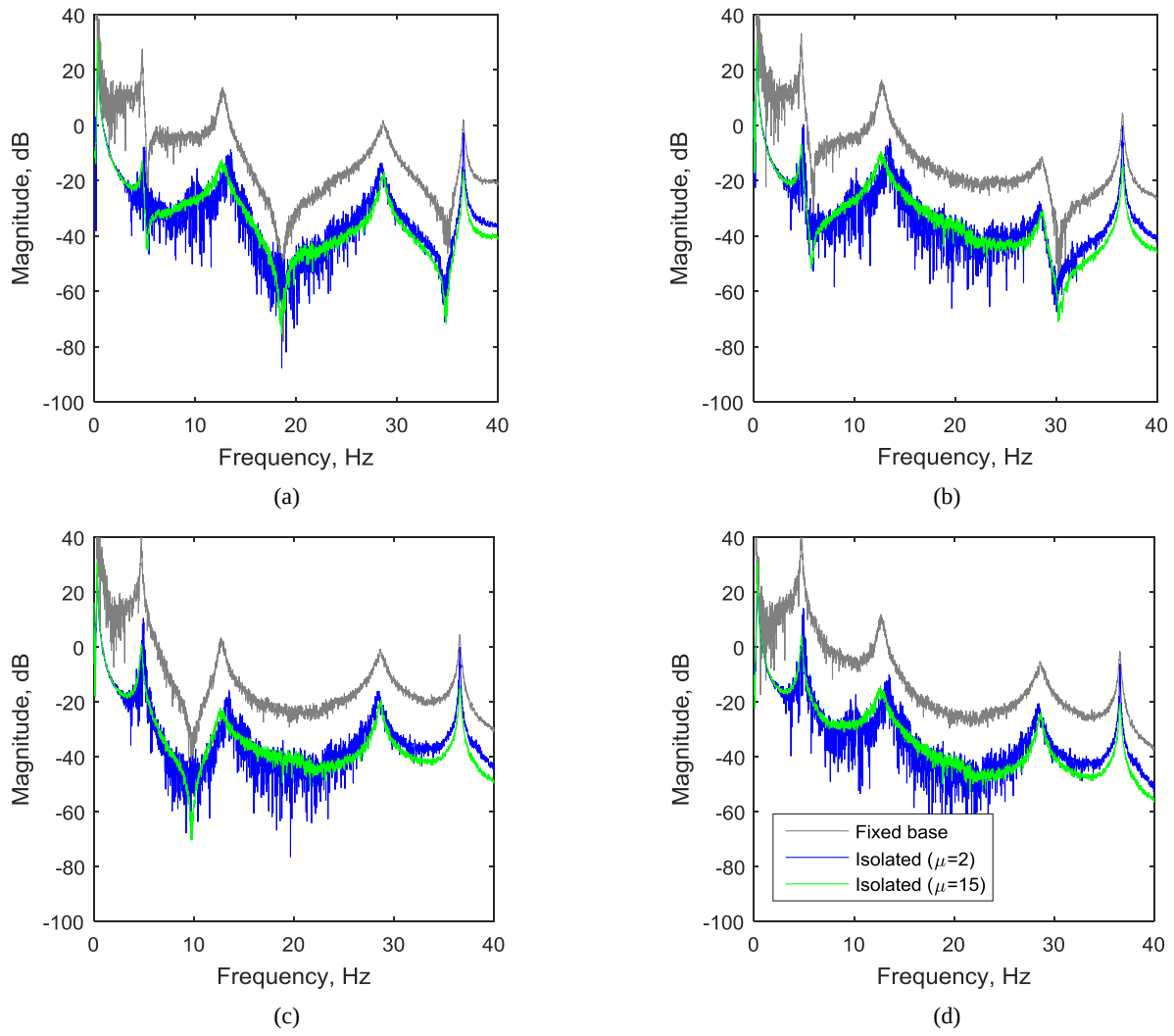

Fig. 13 Experimentally determined transfer functions of absolute story acceleration to ground acceleration for fixed-base and base isolated 4-story buildings: (a) first floor; (b) second floor; (c) third floor; (d) fourth [top] floor

the robust stability and performance margins calculated using the frequency response functions. Fig. 10 shows the performance margins for three different mass ratios (μ = 1, μ = 2, and μ = 15).

Stability and performance analysis results predict that the RTHS test with a mass ratio of one (μ = 1), will not be stable, as the stability margin is above the 0 dB threshold for robust stability around 2 Hz. Using a mass ratio of 2 (μ = 2), the RTHS feedback loop becomes stable, as the stability margin is less than 0 dB however approaches 0 dB near the resonant frequencies of the superstructure and so is not considered to have robust performance. The mass ratio of 15 (μ = 15), provides for both robust stability and performance, as indicted by a performance margin below -20 dB over the bandwidth of interest (0-40 Hz).

4.3 RTHS results

The RTHS tests were conducted at the University of Connecticut. The structure is excited by a band limited white noise excitation with a root mean square (RMS) of 0.125 in and a bandwidth of 0-40 Hz. While it was predicted to be unstable, the RTHS test is first conducted with a mass ratio of 1 (μ = 1). This is done to verify the robust stability and analysis prediction, and done only with sufficient safety measures in place for operators and equipment. Fig. 11 shows a time history of a RTHS test with unstable mass ratio of 1. It is observed that when the mass ratio μ = 1, the RTHS test becomes unstable around 15 seconds, at which time the emergency stop button was activated to shut down the system. Fig. 12 shows time histories of the successfully completed RTHS tests with mass ratios μ = 2 and μ = 15. The RTHS test remains stable over the duration of the test for both of these tests. As described previously these results validate the prediction of the robust stability analysis, namely that the RTHS with μ = 1, system would be unstable and the RTHS tests with μ = 2 and μ = 15 are stable.

The frequency response functions of the superstructure absolute accelerations to input ground acceleration are measured during the RTHS test. Fig. 13 shows the magnitude of the measured frequency response functions for the four stories of the superstructure for three distinct cases: (1) the fixed base structure, the superstructure itself;

(2) the base isolated structure with a mass ratio of 2; and (3) the base isolated structure with a mass ratio of 15.

As observed in Fig. 13, the fixed base structure (superstructure) has resonant frequencies around 5.7 Hz, 13 Hz, 29 Hz and 37 Hz. Also observed in Fig. 9, the isolation reduces the magnitude of the superstructure absolute acceleration response above the isolation frequency by approximately 30 dB (over a 97% reduction) while adding a fifth resonant peak at 0.33 Hz (3 second period), while slightly shifting the frequencies of the resonant frequencies of the superstructure. This is consistent with the results from the analytical study. Further, the resonant peak at the isolation frequency, 0.33 Hz, is increased from 26 to 30 dB, a 4 dB increase similar to that observed in the analytical results. It is also anticipated from the analytical results that while the added mass at the isolation layer should have a minimal effect on the magnitudes and phase of the isolated system above the isolation frequency. What is observed in Fig. 13 is that the frequency response function of the mass ratio 15 is much cleaner than the frequency response function for a mass ratio of 2. The data acquisition and processing for both RTHS tests were the same. As such, the difference can be attributed to the difference between the robust stability (mu = 2) and the robust stability and performance (m = 15). The RTHS test with mass ratio of 2 shows a more lightly damped resonant peak at 36 Hz and a corresponding larger magnitude of the frequency response function, which may lead to inaccurate conclusions in the test regarding performance of the isolation layer at higher frequencies of the superstructure. As such, the robust stability and performance measure can predict not only a stable and successful completion of a RTHS test, but also the performance and accuracy of the test results.

5. Conclusions

In this paper a RTHS shake table test to evaluate the seismic performance of a base isolated building is demonstrated and a robust stability and performance analysis method is proposed to asses, prior to conducting the actual test, the efficacy of the planned RTHS test. The robust stability method is developed, casting the actuator dynamics as a multiplicative uncertainty and applying the small gain theorem to derive the sufficient conditions for robust stability and performance. This analysis method can be used to evaluate the robust stability and performance of the actuator transfer system and the compensation approach for RTHS. The attractive feature of this method is that it accommodates linearized modeled or measured frequency response functions for both the physical substructure and actuator dynamics. This presents a major advancement over previous RTHS stability analysis techniques which assume pure time delay for the actuator dynamics and lumped parameter descriptions or the numerical and physical substructures. The robust stability and performance analysis is applied to a RTHS test conducted at the University of Connecticut on a 4-story seismically excited base isolated building. The isolation layer is numerically modeled, while the superstructure is experimentally tested on a shake table. This partitioning of physical and numerical substructures is challenging for RTHS and can easily result in unstable and inaccurate test results. The proposed robust stability and performance analysis method is demonstrated to predict the unstable RTHS test configuration as well as predict stable results that provide marginal and good experimental results, as observed in the measured frequency response functions. The analysis method has made it possible to conduct RTHS tests for base isolated buildings in a substructuring configuration it has not been realized to date, by identifying in this case the necessary mass ratio necessary to insure stability and performance. The results of RHTS test of the base isolated building are shown to capture the response attenuation and frequency shifting expected in an isolated system. The proposed robust stability and performance analysis method provides a useful tool for pre-test planning and post-test diagnostics of RTHS tests. It is observed that by achieving performance, the experimental test results allow the engineer the tools to make sound conclusions regarding the dynamic performance of the system under study.

References

Ashasi-Sorkhabi, A., Malekghasemi, H. and Mercan, O. (2015), "Implementation and verification of real-time hybrid simulation (RTHS) using a shake table for research and education", *J. Vib. Control*, **21**(8), 1459-1472. https://doi.org/10.1177/1077546313498616

Botelho, R.B., Christenson, R. and Franco, J. (2013), "Exact Stability Analysis for Uniaxial Real-Time Hybrid Simulation of 1-DOF and 2-DOF Structural Systems", *Engineering Mechanics Institute Conference*.

Carrion, J.E. and Spencer, B. (2007), "Model-based strategies for real-time hybrid testing", Report No. NSEL-006; Newmark Structural Engineering Laboratory, Department of Civil and Environmental Engineering, University of Illinois at Urbana-Champaign, Champaign, IL, USA.

Chae, Y., Kazemibidokhti, K. and Ricles, J.M. (2013), "Adaptive time series compensator for delay compensation of servo-hydraulic actuator systems for real-time hybrid simulation", *Earthq. Eng. Struct. Dyn.*, **42**(11), 1697-1715. https://doi.org/10.1002/eqe.2294

Chen, C. and Ricles, J. (2009), "Analysis of actuator delay compensation methods for real-time testing", *Eng. Struct.*, **31**, 2643-2655. https://doi.org/10.1016/j.engstruct.2009.06.012

Chen, C. and Ricles, J. (2010), "Tracking error-based servohydraulic actuator adaptive compensation for real-time hybrid simulation", *J. Struct. Eng.*, **136**(4), 432-440. https://doi.org/10.1061/(ASCE)ST.1943-541X.0000124

Christenson, R. and Lin, Y.Z. (2008), "Real-time hybrid simulation of a seismically excited structure with large-scale magneto-rheological fluid dampers", *Hybrid Simulation Theory, Implementations and Applications*, (Ed. by V.E. Saouma and M.V. Sivaselvan), Taylor and Francis NL, ISBN: 978-0-415-46568-7.

Darby, A.P., Blakeborough, A. and Williams, M.S. (1999), "Real time substructure test using hydraulic actuator", *J. Eng. Mech.*, **125**(10), 1133-1139. https://doi.org/10.1061/(ASCE)0733-9399(1999)125:10(1133)

Dimig, J., Shield, C., French, C., Bailey, F. and Clark, A. (1999), "Effective force testing: a method of siesmic simulation for structural testing", *J. Struct. Eng.*, **125**(9), 1028-1037. https://doi.org/10.1061/(ASCE)0733-9445(1999)125:9(1028)

Gao, X., Castaneda, N. and Dyke, S.J. (2013), "Real time hybrid

simulation: from dynamic system, motion control to experimental error", *Earthq. Eng. Struct. Dyn.*, **42**(6), 815-832. https://doi.org/10.1002/eqe.2246

Gawthrop, P.J., Wallace, M.I., Neild, S.A. and Wagg, D.J. (2007), "Robust real-time substructuring techniques for under-damped systems", *Struct. Control Health Monitor.*, **14**, 591-608. https://doi.org/10.1002/stc.174

Goodwin, G.C., Graebe, S.F. and Salgado, M.E. (2001), *Control System Design*, (2nd Edition), Prentice Hall Inc.

Franklin, G.F., Powell, J.D., Emami-Naeini, A. and Powell, J.D. (2006), *Feedback Control of Dynamic Systems*, (5th Edition), Pearson Prentice Hall, NJ, USA.

Horiuchi, T., Nakagawa, M., Sugano, M. and Konno, T. (1996), "Development of a real-time hybrid experimental system with actuator delay compensation", *Proceedgins of the 11th World Conference on Earthquake Engineering*, Paper No. 660.

Horiuchi, T., Inoue, M., Konno, T. and Namita, Y. (1999), "Real time hybrid experimental system with actuator delay compensation and it's applications to a piping system with energy absorber", *Earthq. Eng. Struct. Dyn.*, **28**(10), 1121-1141. https://doi.org/10.1002/(SICI)1096-9845(199910)28:10<1121::AID-EQE858>3.0.CO;2-O

Kyrychko, Y.N., Blyuss, K.B., Gonzalez-Buelga, A., Hogan, S.J. and Wagg, D.J. (2006), "Real-time dynamic substructuring in a coupled oscillator–pendulum system", *Proceeding of the Royal Society A*, **462**, 1271-1294. https://doi.org/10.1098/rspa.2005.1624

Lin, F., Maghareh, A., Dyke, S.J. and Lu, X. (2015), "Experimental implementation of predictive indicators for configuring a real-time hybrid simulation", *Eng. Struct.*, **101**, 427-438. https://doi.org/10.1016/j.engstruct.2015.07.040

Maghareh, A., Dyke, S.J., Prakash, A. and Bunting, G.B. (2014), "Establishing a predictive performance indicator for real-time hybrid simulation", *Earthq. Eng. Struct. Dyn.*, **43**(15), 2299-2318. https://doi.org/10.1002/eqe.2448

Maghareh, A., Waldbjørn, J.P., Dyke, S.J., Prakash, A. and Ozdagli, A.I. (2016), "Adaptive multi-rate interface: development and experimental verification for real-time hybrid simulation", *Earthq. Eng. Struct.ral Dyn.*, **45**(9), 1411-1425. https://doi.org/10.1002/eqe.2713

Naeim, F. and Kelly, J.M. (1999), *Design of seismic isolated structures*: *from theory to practice*, Wiley, Chichester, England.

Nakashima, M. and Masaoka, N. (1999), "Real time on-line test for MDOF systems", *Earthq. Eng. Struct. Dyn.*, **28**, 393-420. https://doi.org/10.1002/(SICI)1096-9845(199904)28:4<393::AID-EQE823>3.0.CO;2-C

Nakashima, M., Kato, H. and Takaoka, E. (1992), "Development of real-time pseudo dynamic testing", *Earthq. Eng. Struct. Dyn.*, **21**(1), 79-92. https://doi.org/10.1002/eqe.4290210106

Nakata, N. and Stehman, M. (2014), "Compensation techniques for experimental errors in real-time hybrid simulation using shake tables", *Smart Struct. Syst., Int. J.*, **14**(6), 1055-1079. https://doi.org/10.12989/sss.2014.14.6.1055

Ou, G., Ozdagli, A.I., Dyke, S.J. and Wu, B. (2015), "Robust integrated actuator control: experimental verification and real-time hybrid-simulation implementation", *Earthq. Eng. Struct. Dyn.*, **44**(3), 441-460. https://doi.org/10.1002/eqe.2479

Phillips, B.M. and Spencer, B. (2012), "Model-based framework for real-time dynamic structural performance evaluation", NSEL Report No NSEL-031.

Roth, S. and Cheney, D. (2001), Directory of International Earth-Quake Engineering Research Facilities. SRI International Center for Science, Technology and Educational Development Policy Division.

Shi, P., Wu, B., Spencer Jr, B.F., Phillips, B.M. and Chang, C.M. (2015), "Real-time hybrid testing with equivalent force control method incorporating Kalman filter", *Struct. Control Health Monit.*, **23**(4), 735-748. https://doi.org/10.1002/stc.1808

Skinner, R.I., Robinson, W.H. and McVerry, G.H. (1993), *An Introduction to Seismic Isolation*, Wiley, Chichester, England.

Skogestad, S. and Postlethwaite, I. (2005), *Multivariable Feedback Control Analysis and Design*, (2nd Edition), John Wiley and Sons Ltd.

Wallace, M.I., Sieber, J., Neild, S.A., Wagg, D.J. and Krauskopf, B. (2005), "Stability analysis of real-time dynamic substructuring using delay differential equation models", *Earthq. Eng. Struct. Dyn.*, **34**, 1817-1832. https://doi.org/10.1002/eqe.513

Zhang, R., Phillips, B.M., Taniguchi, S., Ikenaga, M. and Ikago, K. (2017), "Shake table real-time hybrid simulation techniques for the performance evaluation of buildings with inter-story isolation", *Struct. Control Health Monitor.*, **24**(10), e1971. https://doi.org/10.1002/stc.1971

BS